

# Changes in the long term intensity variations in Cyg X-2 and LMC X-3

B. Paul<sup>1,3</sup>, S. Kitamoto<sup>2</sup> and F. Makino<sup>1</sup>

<sup>1</sup>*Institute of Space and Astronautical Science, 3-1-1 Yoshinodai, Sagamihara, Kanagawa 229-8510, Japan*

<sup>2</sup>*Department of Earth and Space Science, Faculty of Science, Osaka University 1-1, Machikaneyama, Toyonaka, Osaka, 560, Japan*

*e-mail: bpaul@astro.isas.ac.jp, kitamoto@ess.sci.osaka-u.ac.jp, makino@astro.isas.ac.jp*

## ABSTRACT

We report the detection of changes in the long term intensity variations in two X-ray binaries Cyg X-2 and LMC X-3. In this work, we have used the long term light curves obtained with the All Sky Monitors (ASM) of the Rossi *X-ray Timing Explorer (RXTE)*, *GINGA*, *ARIEL 5* and *VELA 5B* and scanning modulation collimator of *HEAO 1*. It is found that in the light curves of both the sources, obtained with these instruments at various times over the last 30 years, more than one periodic or quasi-periodic components are always present. The multiple prominent peaks in the periodograms have frequencies unrelated to each other. In Cyg X-2, *RXTE-ASM* data show strong peaks at 40.4 and 68.8 days, *GINGA-ASM* data show strong peaks at 53.7 and 61.3 days. Multiple peaks are also observed in LMC X-3. The various strong peaks in the periodograms of LMC X-3 appear at 104, 169 and 216 days with *RXTE-ASM*, and 105, 214 and 328 days with *GINGA-ASM*. The present results, when compared with the earlier observations of periodicities in these two systems, demonstrate the absence of any stable long period. The 78 day periodicity detected earlier in Cyg X-2 was probably due to the short time base in the *RXTE* data that were used and the periodicity of 198 days in LMC X-3 was due to a relatively short duration of observation with *HEAO 1*.

*Subject headings:* accretion, accretion disks – stars: individual (Cyg X-2, LMC X-3) – stars: neutron – X-rays: binaries

---

<sup>3</sup>On leave from the Tata Institute of Fundamental Research, Homi Bhabha Road, Mumbai, 400005, India

## 1. Introduction

Many X-ray binaries are highly variable in their X-ray intensity over long time scales. But in most of the sources, either the intensity variations are aperiodic or their periodic nature has not yet been discovered because of long-period, low modulation or a lack of sensitive uninterrupted monitoring. The All Sky Monitor (ASM) onboard the Rossi *X-ray Timing Explorer* (*RXTE*) has produced light curves of many bright X-ray binaries for about 1,000 days with large signal to noise ratio. The *RXTE-ASM* data along with the *GINGA-ASM*, *VELA 5B*, *ARIEL 5* and *HEAO 1* data have a large time base and it is possible not only to search for any periodic or quasi periodic intensity variations of a few days to a few months time scale, but also to investigate changes in the timing behaviour. Changes in the long term periodicity have been observed in SMC X-1 (Wojdowski et al. 1998) and GX 354-0 (Kong et al. 1998). We selected Cyg X-2 and LMC X-3 to study any possible changes in the long term periodicity because in these two sources long term periodicity is known to exist in data bases covering a very long time and also for the fact that light curves for the intervening period 1987–1991 were available from the *GINGA-ASM*.

Cyg X-2, a bright X-ray source, was discovered by Byram et al. (1966) with a sounding rocket experiment. A binary period of 9.8 days, other orbital parameters and mass limits of the two components of this binary system were measured by Cowley et al. (1979). This is a low mass X-ray binary and a typical Z source that shows Type-I X-ray bursts (Kahn & Grindlay 1984; Smale 1998), 18–50 Hz QPOs in the horizontal branch and 5.6 Hz QPOs in the nominal branch (Hasinger et al. 1986; Elsner et al. 1986; Wijnands et al. 1997; Kuulkers, Wijnands and van der Klis 1999). Recently, with the *RXTE*, kHz QPOs with two peaks have also been detected from this source (Wijnands et al. 1998). Vrtilik et al. (1988) discovered X-ray dips of different types and some were found to occur in one particular phase of the binary period. A 77 day periodicity was discovered from the *VELA 5B* observations (Smale & Lochner 1992). Wijnands, Kuulkers & Smale (1996) reported detection of a periodicity of 78 days from the first 160 days of ASM data, and showed that their result was supported by the archival data of *ARIEL 5* and *VELA 5B*.

LMC X-3, a high mass X-ray binary, was discov-

ered with the *UHURU* satellite (Leong et al. 1971) and its position was measured accurately with the *HEAO 1* scanning modulation collimator (Johnston et al. 1978). From spectroscopic observations Cowley et al. (1983) discovered an orbital period of 1.7 days and a mass function of  $2.3 M_{\odot}$ . LMC X-3 is considered to be a very strong black hole candidate (BHC) due to the fact that the mass of the compact object has a lower limit of  $9 M_{\odot}$ . But, *HEAO A2* observations revealed that unlike other known black hole candidates, LMC X-3 lacks rapid X-ray variability (Weisskopf et al. 1983). The lowest time scale for 1% rms amplitude variation was derived from the *EXOSAT* observations to be 600 s (Treves et al. 1988). One possible explanation for the lack of rapid X-ray variability is that most of the time LMC X-3 is found to be in a high state with an unusually soft X-ray spectrum (White & Marshal 1984), and the rapid X-ray variations are generally subdued in Cyg X-1 like BHCs in their high state. *GINGA* observations showed that the energy spectrum consists of a soft, thermal component and a hard, power-law component. In spite of large changes in mass accretion rate and disk temperature, the inner radius of the accretion disk was found to be remarkably constant and was suggested to be related to the mass of the compact object (Ebisawa et al. 1993). Long term intensity variation is well known in LMC X-3 and Cowley et al. (1991) discovered a periodicity of 198 (or 99) days from the *HEAO A1* and *GINGA* large area counter data.

The light curves of Cyg X-2 and LMC X-3 obtained with the ASMs onboard the *RXTE*, *GINGA*, *VELA 5B* (only for Cyg X-2), *ARIEL 5* and the scanning modulation collimator of the *HEAO 1* (only for LMC X-3) have been used to investigate the long term intensity variations in these two sources and we have found presence of multiple components of flux variations in both the sources. The data used here together covers a time base of 30 years for Cyg X-2 and 26 years for LMC X-3.

## 2. Data and analysis

The ASM on board *RXTE* scans the sky in a series of dwells of about 90 s each, and any given X-ray source is observed in about 5–10 such dwells every day. The details about the ASM detectors and observations with the ASM are given in Levine et al. (1996). We have used the quick look ASM data obtained in the period 1996 February 20 to 1999 Febru-

ary 4, provided by the *RXTE-ASM* team. The ASM data are available in two different forms, per dwell and one day average. The periodograms obtained from the two sets of data are identical except for a normalization. Hence the results obtained from the one day average data are presented here. The *GINGA-ASM* was operational during 1987 to 1991 and details of the detectors, operations, and the detection techniques have been described by Tsunemi et al. (1989). The all sky observations were performed about once every day when the satellite was given one full rotation with about 70% sky coverage by the ASM. The detection limit in one such rotation was of the order of 50 mCrab and was dependent on the position of the source with respect to the satellite equator. Archival data of *VELA 5B* and *ARIEL 5* were obtained from the HEASARC data base and *HEAO 1* data for LMC X-3 were taken from previously published work (Cowley et al. 1991). For details about the *ARIEL 5* ASM and the *VELA 5* instrument please refer to Holt (1976) and Priedhorsky, Terrel & Holt (1983) respectively.

To search for periodicities in the unevenly sampled data, we have used the method suggested by Lomb (1976) & Scargle (1982). For Cyg X-2, we generated periodograms in the period range of 10–160 days from the *RXTE-ASM*, *GINGA-ASM*, *ARIEL 5* and *VELA 5B* data. The *ARIEL 5*, *VELA 5B* and initial part of the *RXTE-ASM* light curves were analyzed earlier and long periods of 78 and 69 days were reported (Smale & Lochner 1992; Wijnands et al. 1996, Kong et al. 1998). For LMC X-3, light curves from *RXTE-ASM*, *GINGA-ASM*, *ARIEL 5* and *HEAO 1* were used to generate periodogram in the range of 20–500 days. *VELA 5B* data for LMC X-3 has low signal to noise ratio and is not used here. The discovery of a 198 (or 99) day periodicity from the *HEAO 1* light curve was made by Cowley et al. (1991), and the initial part of the *RXTE-ASM* data also showed similar variation (Wilms et al. 1998). The period ranges chosen for the periodogram analysis are such that a sub-harmonic or first harmonic of the earlier known periods can be identified for the respective sources. For Cyg X-2, we also verified that in the 160-500 days range the periodograms generated from data sets are featureless except for *ARIEL 5* which shows peaks around 180 and 360 days due to known yearly effect (Priedhorsky et al. 1983).

The significance of the various peaks detected in the periodograms is given in Table 1 in terms of the

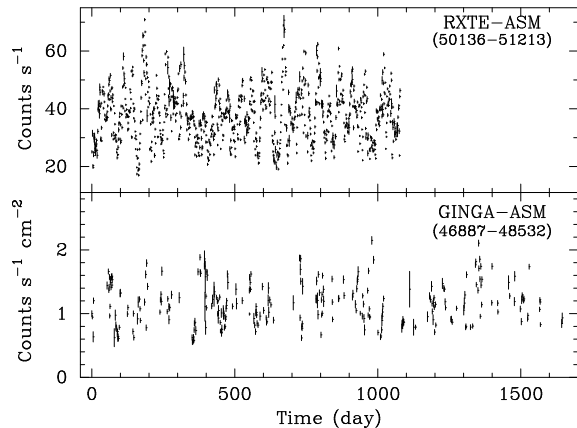


Fig. 1.— The *RXTE-ASM* (1.5–12 keV) and *GINGA-ASM* (1–20 keV) light curves of Cyg X-2. The days of the observations are given in truncated Julian days in the figure.

false alarm probability (FAP) calculated following the method suggested by Horne & Baliunas (1986). The window functions, which can induce artificial periodicities were calculated for the different time series used here. The *GINGA-ASM* time series, which is very susceptible to artificial periodicities because of its scarce sampling, does not show any alarming feature in the period range used in this paper and the effect of the window function is less for the other instruments. However, we wish to point out that the use of window function to find spectral leakage can sometimes be misleading for this kind of light curves. As an example, in the *HEAO 1* light curve of LMC X-3, the density of data points available is larger when the source is brighter, and this is likely to be true for other sources and instruments also. This results in some features in the window function at periods near 80 and 160 days, whereas a glance at the light curve (Figure 4) leaves no doubt about the presence of a periodic variation. We have verified the significance of the peaks in the periodograms independently using two more methods. Following Kong et al. (1998), we have generated light curves using random numbers, with the time series, average, and variance similar to the real light curves and calculated the periodograms for 10,000 such light curves. The highest points in these periodograms were identified and a power which is larger than the highest points of 99% of the periodograms is considered to correspond to a false alarm probability of  $10^{-2}$ . The same process was carried out also for 10,000 light curves with the same time

series as the real light curves, but the count rates redistributed randomly. The results from these two analysis are found to be identical and the  $10^{-2}$  false alarm levels are indicated by dashed lines in all the periodograms. Absence of strong peaks in the periodograms calculated from the simulated and redistributed light curves confirms that the peaks observed in the periodograms of the real light curves are not artifact of observation windows.

## 2.1. Cyg X-2

Presence of strong intensity variations by a factor of  $\sim 2-4$  on time scale of weeks is well known in this source (Kuulkers, van der Klis, & Vaughan 1996; Wijnands et al. 1996) and can be clearly seen in the light curves of *RXTE-ASM* and *GINGA-ASM* (Figure 1). A periodic nature of this intensity variation with period of less than 100 days is also apparent in the light curves.

The periodograms obtained from the *RXTE-ASM*, *GINGA-ASM*, *ARIEL 5* and *VELA 5B* data are shown in Figure 2. In the *RXTE-ASM* data, there are several significant peaks and the two most prominent ones are at 40.4 and 68.8 days indicating the presence of multiple periodicities in this system. In the *GINGA-ASM* periodogram there are two prominent peaks at 53.7 and 61.3 days and there are several smaller peaks. The periodogram of the *ARIEL 5* data is a very complicated one and has many prominent peaks at frequencies ranging between 30 and 80 days. In addition to the 78 days peak noticed by Wijnands et al. (1996), there are other peaks at 41, 46 and 54 days. The *VELA 5B* data has low signal to noise ratio and the power in the periodogram is much smaller, but two peaks at 33.9 and 77.4 days can be clearly seen in Figure 2. The significance of the peaks detected in various periodograms are given in Table 1.

To investigate whether these multiple peaks in the periodograms originate in different parts of the light curves or whether multiple peaks are present throughout the entire light curve of each satellite, we have divided the light curves of *RXTE* and *ARIEL 5* into three equal segments and generated periodograms from each of them. There are several prominent peaks in each of the periodograms, and the periods of these peaks are noted in Table 1 along with the significance of their detection. Periodograms obtained from the three 358 day segments of the *RXTE* light curve are shown in Figure 3 along with the respective light

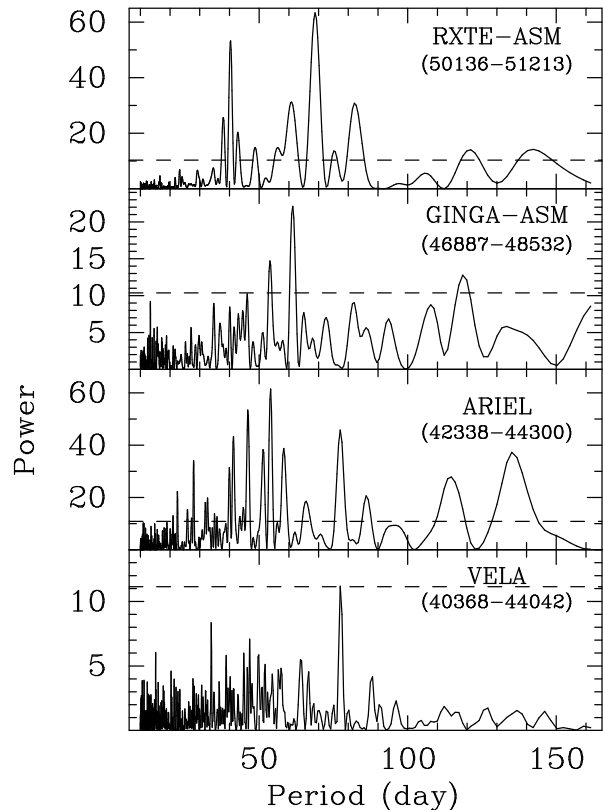


Fig. 2.— The Lomb-Scargle periodograms obtained from the *RXTE-ASM*, *GINGA-ASM*, *ARIEL 5* and *VELA 5B* light curves of Cyg X-2. The horizontal dashed line represent the 99% confidence limits (see text for details).

curves. It is evident from Figure 3 and Table 1 that there are multiple periodicities in this system that are uncorrelated and have varying amplitude and period. The higher frequency variation at around 40 days time scale appears to be more stable in frequency than the lower frequency variations around 70 days during these observations.

## 2.2. LMC X-3

Long term light curves of LMC X-3, obtained with the *RXTE-ASM*, *GINGA-ASM* and HEAO 1 are shown in Figure 4. The HEAO 1 data, plotted in the lower panel of the figure, very clearly shows almost periodic intensity variations at about 100 days. However, as Cowley et al. (1991) pointed out, the intensity modulation is missing during the first 100 days. They concluded from this data that the intensity vari-

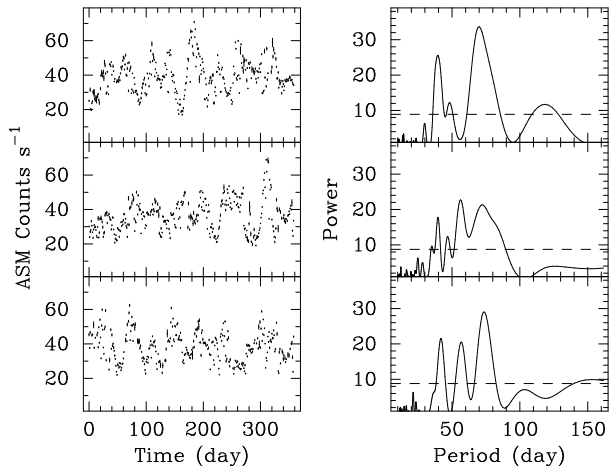


Fig. 3.— Three segments of the *RXTE-ASM* light curve of length 358 days each and the corresponding Lomb-Scargle periodograms are shown on the left and right hand sides respectively. The 99% confidence limits are shown with the dashed horizontal lines.

ations in LMC X-3 is periodic at  $\sim 198$  (or possibly  $\sim 99$ ) days. The *GINGA-ASM* light curve shown in the middle panel of the figure also indicates intensity modulations, but at a larger time scale of about 200 days. Two such modulations can be clearly identified at the end of the light curve and one more in the middle. There are also some episodes of about 100 days periodic variations in some parts of the *GINGA-ASM* light curve. The *RXTE-ASM* light curve of LMC X-3, as shown in the top panel of Figure 4, shows a varying nature of the approximately 100 or 200 days intensity variations. At the beginning, there are three strong modulations at about 100 days, similar to what was seen with *HEAO 1*, but in the later part of the light curve, the modulations are much less prominent and have larger time scale. Intensity variations in LMC X-3 are not clearly visible in the *ARIEL 5* light curve (not shown here) because of sparse sampling.

In Figure 5 we have shown the periodograms generated from the light curves of LMC X-3 obtained with all the four satellites mentioned above. There are three prominent peaks at 104.4, 168.8 and 215.6 days in the periodogram obtained from the *RXTE-ASM* light curve. The peak at 104.4 days is narrow while the other two are broad. In the periodogram of the *GINGA-ASM*, however, there are two prominent peaks at 214 and 328 days. There is also a less significant indication of some periodic component at 105 days. The *HEAO 1* data which have been extensively

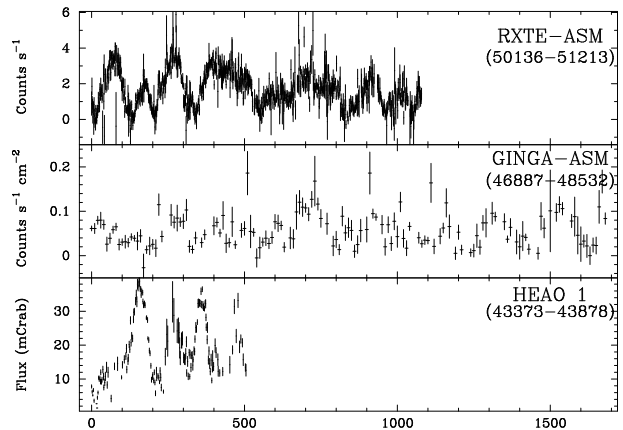


Fig. 4.— The long term light curves of LMC X-3 obtained with the *RXTE-ASM*, *GINGA-ASM* and *HEAO 1* satellites. The energy ranges are 1.5–12 keV, 1–20 keV and 1–13 keV respectively.

discussed by Cowley et al. (1991), predictably shows two peaks at 99 and 203 days with the former being narrower. Results from the *RXTE* and *HEAO 1* are similar in nature except for the fact that the broad peak near 200 days is resolved into two components in the *RXTE-ASM* data. This also shows that the two peaks near 100 and 200 days as seen in the periodogram of the *HEAO 1* data are not related. The periodogram of the *GINGA-ASM* light curve also has a shape similar to the other two but the time scale is a factor of two larger. The *ARIEL 5* light curve has low signal to noise ratio and infrequent sampling and the periodogram obtained from this data shows three less significant peaks at 90, 96 and 130 days. At periods below 50 days, this periodogram is very noisy. From the four periodograms shown in Figure 5 it appears that there is a quasi periodic component at around 100 days in LMC X-3 whose strength is time dependent. There is at least one more component at longer period of about 200 days. The period excursion of the  $\sim 100$  days component is significant, but relatively smaller than the other periodicities.

To investigate the nature of the multiple components of intensity variations in more detail, we have done further analysis of the *RXTE-ASM* data of LMC X-3 in a manner similar to what was done with the Cyg X-2 data. We divided the light curve into two segments, each 540 days long, and have generated the periodograms from both of the segments that are shown in Figure 6. Two large peaks at 104.3 and 177.8 days are clearly seen in the first periodogram

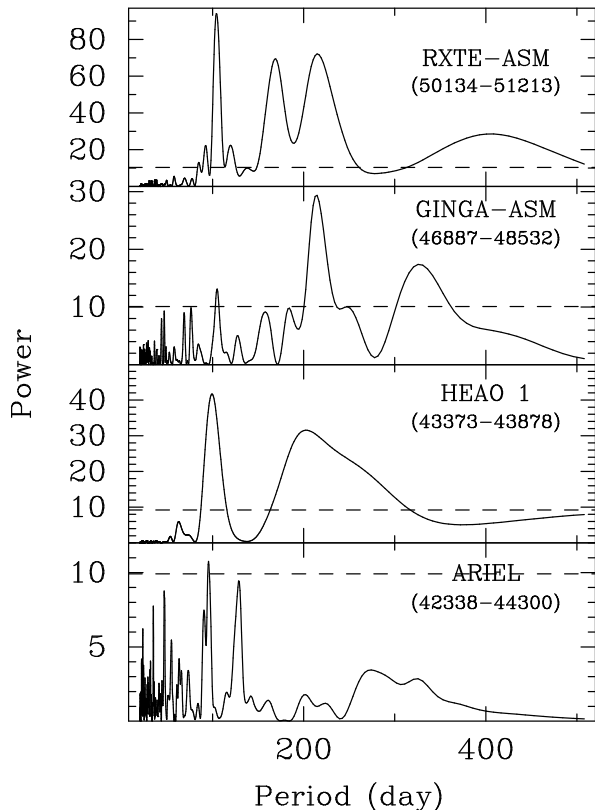


Fig. 5.— The Lomb-Scargle periodograms generated from the light curves of LMC X-3 obtained with the *RXTE-ASM*, *GINGA-ASM*, *HEAO 1* and *ARIEL 5* detectors. The dashed horizontal lines indicate the 99% confidence limits.

whereas the periodogram generated from the second part of the light curve shows two peaks at 101.9 and 221.6 days with much less strength. It appears that the  $\sim 104$  day periodicity is suppressed in the second part of the *RXTE* data and the second component of intensity variation has moved to a longer time scale. The significance of the peaks in the periodograms are given in Table 1.

### 2.3. Spectral variations

In Cyg X-2, the hardness ratio and intensity that define its position in the Z track and also the position of the Z track itself, changes significantly at short time scales. But at longer time scales, in between different observations, a negative correlation was found between the hardness ratio and total intensity with *EXOSAT* (Kuulkers et al. 1996), *GINGA* (Wijnands et al. 1997) and also with the *RXTE-ASM* during its

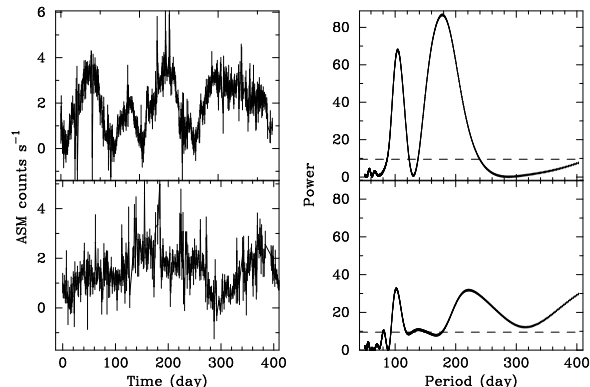


Fig. 6.— The Lomb-Scargle periodograms obtained from two segments of the *RXTE-ASM* light curve of LMC X-3. Each segment of the light curve is of 540 days duration. The dashed horizontal lines indicate the 99% confidence limits.

first few months observations (Wijnands et al. 1996). The hardness ratio in LMC X-3, on the other hand was found to have positive correlation with intensity (Cowley et al. 1991). We have calculated the two hardness ratios HR1 (3.0-5.0 keV/1.5-3.0 keV) and HR2 (5.0-12 keV/3.0-5.0 keV) from the *RXTE-ASM* data as a function of the total intensity for the two sources (Figure 7) using all the available data. In Cyg X-2, HR2 is negatively correlated with luminosity (correlation coefficient -0.6 and probability of no correlation  $10^{-30}$ ) but HR1 does not show any correlation (coefficient -0.04, probability 0.5). If the data points are connected by lines, the HR2 plot appears like a loop indicating that HR2 follows two different tracks during the rising and decaying phases of the intensity variations. Large deviation in the hardness plot of Cyg X-2 is due to movement of the source along the Z track (Wijnands et al. 1996) and changing position of the Z track in the color-color diagram. In LMC X-3, a weak positive correlation is found for HR1 (0.5,  $10^{-5}$ ) but no correlation for HR2 (-0.07, 0.5). The correlation coefficients and probabilities were calculated using two different methods: the linear and rank correlation, both gave identical results.

### 3. Discussion

Apart from the binary period, long term periodic variations are known to be present in many X-ray binaries. There are four sources in which the presence of long periods is very well established, (1) Her X-1,

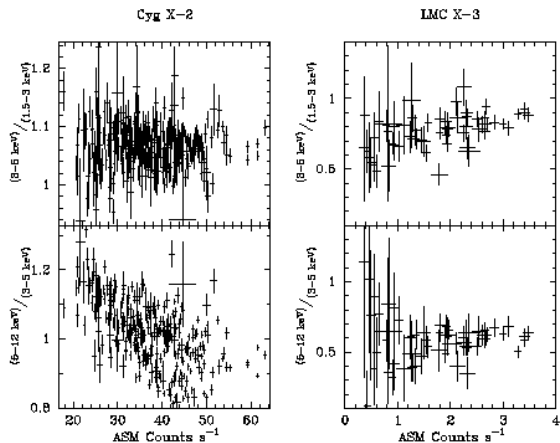


Fig. 7.— Hardness ratios HR1 (3-5 keV / 1.5-5 keV) and HR2 (5-12 keV / 3-5 keV) of Cyg X-2 and LMC X-3 obtained from the *RXTE-ASM* data are plotted against the total intensity. Cyg X-2 data points are averaged for 3 days and LMC X-3 data points are averaged for 10 days.

a 1.7 day binary with a 35 day period (Giacconi et al. 1973), (2) LMC X-4, a 1.4 day binary with a 30.5 day period (Lang et al. 1981), (3) SMC X-1, a 3.9 day binary with a long period of 60 days (Wojdowski et al. 1998) and (4) SS 433, a 13.1 day binary with a long period of 164 days (Margon et al. 1979). Incidentally, the first three of these sources are also X-ray pulsars. In SS 433, the periodicities are detected photometrically and spectroscopically in the optical band only. There is also evidence of periodic component in several other sources. Among the high mass X-ray binaries, periodicity has been observed in Cyg X-1 at 300 days (Priedhorsky et al. 1983, also see Kitamoto et al. (1999) for the *GINGA-ASM* observations of a  $\sim 150$  day period), 4U 1907+09 at 42 days (Priedhorsky & Terrell 1984) and LMC X-3 at 198 (or 99) days (Cowley et al. 1991). Among the low mass X-ray binaries, Smale & Lochner (1992) found periodicity in three sources, Cyg X-2 (78 days), 4U 1820-303 (175 days) and 4U 1916-053 (199 days). A 106 day periodicity was discovered from an extragalactic point source in the spiral galaxy M33 (Dubus et al. 1997). The *RXTE-ASM* observations of a large number of sources, for the past three years, detected intensity variations in many sources (see Levine 1998 for a summary and the light curves). Some of these sources are of periodic nature and there has also been discovery

of new periodic sources using the *RXTE-ASM* data (Sco X-1, Peele & White 1996; X2127+119, Corbet, Peele & Smith 1996). Unstable long-term periodicity that is attributed to activity of the companion star or instability of the accretion disk has been observed in Aql X-1 (Kitamoto et al. 1993). The ratio of the long and orbital periods in these sources has a wide range between 5 (in 4U 1907+09) and 22,000 in (4U 1820-303). In the two binaries Cyg X-2 and LMC X-3, the reported long term periodicity is larger by a factor of 8 and 116 than the respective orbital periods.

The long periods in Her X-1, LMC X-4 and SS 433 are believed to be produced by the precession of the accretion disks. The mechanisms proposed to cause the precession of the disks are, (1) forced precession of a tilted disk by the gravitational field of the companion star (Katz 1973) and (2) precession of a disk that is slaved to a misaligned companion star (Roberts 1974). But, the time scale of precession expected in the sources in which binary parameters are well known is in disagreement with the observed long periods (Priedhorsky & Holt 1987). One additional problem is that a large excursion is observed in the long period of Her X-1 (Ögelman 1985) and SS 433 (Margon 1984), and it may also be present in LMC X-4. This is not explained in the above two models of disk precession (see Priedhorsky & Holt 1987, for a detailed discussion). However, in a realistic case, when various factors like magnetic pressure, radiation pressure, tidal force, relativistic frame dragging etc. are considered, it is possible to have significant deviation in the precession period from its time averaged value. Recent developments in the models, including tilted and twisted disks due to coronal winds (Schandl & Meyer 1994; Schandl 1996) and warped precessing disks due to radiation pressure (Maloney, Begelman & Pringle 1996; Wijers & Pringle 1998) have a provision for variations in the precession period. Other models have also been considered to explain the long periods. These are 1) precession of the compact object (Trümper et al. 1986), 2) influence of a third body (Fabian et al. 1986) and 3) periodic modulation of the mass accretion rate (Priedhorsky & Holt 1987). Among these models, the first one is not applicable for black hole sources, and the second one appears to be not true for the two pulsars Her X-1 (Tananbaum et al. 1972) and LMC X-4 (Pietsch et al. 1985). In Her X-1 and LMC X-4, the presence of a third body required to produce the long period, would have resulted in additional detectable varia-

tions in the pulsation property (Priedhorsky & Holt 1987). Periodic and asymmetric mass transfer, which is induced by the disk's shadowing of the Roche-lobe overflow region, also contributes to the slaved nature of the accretion disk and is a possible mechanism. Mass transfer feedback induced by X-ray irradiation may also generate the observed long term periodicities (Osaki 1985).

No clear understanding of the reason behind the observed long-term periodicities stands out among all these possibilities. None of the possibilities mentioned above can explain the long-term periodicity in all the sources. In the high mass X-ray binaries, the periodicity is generally believed to be related to disk precession and in the low mass X-ray binaries another possibility is some type of disk instability or modulation in the mass accretion rate related to or induced by the X-ray radiation (Meyer 1986).

Varying obscuration by the disk (caused by precession), which provides a good explanation for the long term periodicity, should have the following observational consequence. With increased absorption in the low intensity phase, a hardening in the spectrum is expected which is known to be present in Her X-1 and LMC X-4. The spectral hardening is likely to be more pronounced between the two lower energy bands. Contrary to this expectation, we find that in Cyg X-2, HR1 is uncorrelated to the total intensity whereas HR2 is anti-correlated, and in LMC X-3, HR1 has a weak positive correlation (Figure 7). Therefore, the spectral variations do not provide very good support to the disk obscuration scenario.

The present work involving light curves of these two sources with very large time base suggests that there is no stable periodicity in either of these systems. There are indications that the oscillatory components seen in the light curves have varying amplitude and period. Forced or slaved precession of the accretion disk is unlikely to be the mechanism behind the quasi periodic intensity variations observed here. Scenarios including disk precession induced by radiation pressure or tilted and twisted disk structure induced by wind also require spectral variations different from the observed pattern. The presence of a third body is also likely to produce more regular patterns in the intensity variations. Another plausible explanation for the observed behaviour is instability in the disk or in the mass accretion rate. But Kuulkers et al. (1996) have pointed out that changes in the mass accretion rate is unlikely to produce the

long term behaviour observed in Cyg X-2, because changes in the mass accretion rate on a time scale of less than a day and associated spectral changes are in fact known to produce the Z pattern (Hasinger & van der Klis 1989).

However, if we look only at the *RXTE* ASM data of Cyg X-2 (Figure 3), it appears that there are two unrelated components of intensity variations at periods of  $\sim 40$  and  $>60$  days, with the first component more stable in period than the second one. The results obtained from LMC X-3 (Figures 5 and 6) is somewhat similar with a relatively stable component at  $\sim 100$  days and a highly varying component at  $>130$  days. It is possible that in both objects there are two sources of intensity variation, the first one relatively stable with a smaller period caused by precession of the accretion disk or by a third body and the second one unstable in time and having a longer time scale caused by disk instability or changes in the mass accretion rate. Coupling between the two components may result in incorrect measurement of the period of the first component.

We thank an anonymous referee for many suggestions which helped to improve a previous version of the manuscript. This research has made use of data obtained through the High Energy Astrophysics Science Archive Research Center Online Service, provided by the NASA/Goddard Space Flight Center. We also thank the *RXTE-ASM* and *GINGA-ASM* teams for providing the valuable data. B. Paul was supported by the Japan Society for the Promotion of Science through a fellowship.

## REFERENCES

- Byram, E. T., Chubb, T. A., & Friedman, H. 1966, *Science*, 152, 66
- Corbet, R., Peele, A., & Smith, D. A. 1996, *IAUC*, 6632
- Cowley, A. P., Crampton, D., & Hutchings, J. B. 1979, *ApJ*, 231, 539
- Cowley, A. P., Crampton, D., Hutchings, J. B., Remillard, R., & Penfold, J. E. 1983, *ApJ*, 272, 118
- Cowley, A. P., et al. 1991, *ApJ*, 381, 526
- Dubus, G., Charles P. A., Long, K. S., & Hakala, P. J. 1997, *ApJ*, 490, L47

- Ebisawa, K., Makino, F., Mitsuda, K., Belloni, T., Cowley, A. P., Schmidtke, P. C., & Treves, A. 1993, *ApJ*, 403, 684
- Elsner, R. F., Weisskopf, M. C., Darbro, W., Ramsey, B. D., Williams, A. C., Sutherland, P. G., & Grindlay, J. E. 1986, *ApJ*, 308, 655
- Fabian, A. C., Eggleton, P. P., Pringle, J. E., & Hut, P. 1986, *ApJ*, 305, 333
- Giacconi, R., Gursky, H., Kellogg, E., Levinson, R., Schreier, E., & Tananbaum, H. 1973, *ApJ*, 184, 227
- Hasinger, G., Langmeier, A., Sztajno, M., Truemper, J., & Lewin, W. H. G. 1986, *Nature*, 319, 469
- Hasinger, G., & van der Klis, M. 1989, *A&A*, 225, 79
- Holt, S. S., 1976, *Ap&SS*, 42, 123
- Horne, J. H., & Baliunas, S. L. 1986, *ApJ*, 302, 757
- Johnston, M. D., Bradt, H. V., Doxsey, R. E., Gursky, H., Schwartz, D. A., Schwarz, J., & van Paradijs, J. 1978, *ApJ*, 225, L59
- Kahn, S. M., & Grindlay, J. E. 1984, *ApJ*, 281, 826
- Katz, J. I. 1973, *Nature*, 246, 87
- Kitamoto, S., Egoshi, W., Miyamoto, S., Tsunemi, H., Ling, J. C., Wheaton, W. A., & Paul, B. 2000, *ApJ* (in press)
- Kitamoto, S., Tsunemi, H., Miyamoto, S., & Roussel-Dupre, D. 1993, *ApJ*, 403, 315
- Kong, A. K. H., Charles, P. A., & Kuulkers, E. 1998, *New Astronomy*, 3, 301
- Kuulkers, E., van der Klis, M., & Vaughan, B. A. 1996, *A&A*, 311, 197
- Kuulkers, E., Wijnands, R., & van der Klis, M. 1999, *MNRAS*, 308, 485
- Lang, F. L., et al. 1981, *ApJ*, 246, L21
- Leong, C., Kellogg, E., Gursky, H., Tananbaum, H., & Giacconi, R. 1971, *ApJ*, 170, L67
- Levine, A. M. 1998, in "The Active X-ray Sky; results from BeppoSAX and Rossi-XTE", *Nuclear Physics B*, (Proc. Suppl.), 69/1-3, 196
- Levine, A. M., Bradt, H., Cui, W., Jernigan, J. G., Morgan, E. H., Remillard, R., Shirey, R. E., & Smith, D. A. 1996, *ApJ*, 469, L33
- Lomb, N. R. 1976, *Ap&SS*, 39, 447
- Maloney, P. R., Begelman, M. C., & Pringle, J. E. 1996, *ApJ*, 472, 582
- Margon, B. 1984, *ARA&A*, 22, 507
- Margon, B., Grandi, S. A., Stone, R. P. S., & Ford, H. C. 1979, *ApJ*, 233, L63
- Meyer, F., in "Radiation Hydrodynamics in Stars and Compact Objects", *Proceedings of IAU Colloq. 89*, 1986, Eds. D. Mihalas & Karl-Heinz A. Winkler, Springer-Verlag, P. 249, 1986
- Ögelman, H., Kahabka, P., Pietsch, W., Trümper, J., & Voges, W. 1985, *SSRv*, 40, 3470
- Osaki, Y. 1985, *A&A*, 144, 369
- Peele, A. G., & White, N. E. 1996, *IAUC*, 6524
- Pietsch, W., Voges, W., Pakull, M., & Staubert, R. 1985, *SSRv*, 40, 371
- Priedhorsky, W. C., & Holt, S. S. 1987, *SSRv*, 45, 291
- Priedhorsky, W. C., & Terrell, J. 1984, *ApJ*, 280, 661
- Priedhorsky, W. C., Terrell, J., & Holt, S. S. 1983, *ApJ*, 270, 233
- Roberts, W. J. 1974, *ApJ*, 187, 575
- Schandl, S. 1996, *A&A*, 307, 95
- Schandl, S., & Meyer, F. 1994, *A&A*, 289, 149
- Scargle, J. D. 1982, *ApJ*, 263, 835
- Smale, A. P. 1998, *ApJ*, 498, L141
- Smale, A. P., & Lochner, J. C. 1992, *ApJ*, 395, 582
- Tananbaum, H., Gursky, H., Kellogg, E., Giacconi, R., & Jones, C. 1972, *ApJ*, 177, L5
- Treves, A., Belloni, T., Chiappetti, L., Maraschi, L., Stella, L., Tanzi, E. G., & van Der Klis, M. 1988, *ApJ*, 325, 119
- Trümper, J., Kahabka, P., Ögelman, H., Pietsch, W., Voges, W. 1986, *ApJ*, 300, L63

- Tsunemi, H., Kitamoto, S., Manabe, M., Miyamoto, S., Yamashita, K., & Nakagawa, M. 1989, PASJ, 41, 391
- Vrtilek, S. D., Swank, J. H., Kelley, R. L., & Kahn, S. M. 1988, ApJ, 329, 276
- Weisskopf, M. C., Darbro, W. A., Elsner, R. F., Williams, A. C., Kahn, S. M., Grindlay, J. E., Naranan, S., & Sutherland, P. G. 1983, ApJ, 274, L65
- White, N. E., & Marshall, F. E. 1984, ApJ, 281, 354
- Wijers, R. A. M. J., & Pringle, J. E.. 1999, MNRAS, 308, 207
- Wijnands, R. A. D., Kuulkers, E., & Smale A. P. 1996, ApJ, 473, L45
- Wijnands, R., Homan, J., van Der Klis, M., Kuulkers, E., van Paradijs, J., Lewin, W. H. G., Lamb, F. K., Psaltis, D., & Vaughan, B. 1998, ApJ, 493, L87
- Wijnands, R. A. D., van der Klis, M., Kuulkers, E., Asai, K., & Hasinger, G. 1997, A&A, 323, 399
- Wilms, J., Nowak, M. A., Dove, J. B., Pottschmidt, K., Heindl, W. A., Begelman, M. C., & Staubert, R. 1999, in Highlights in X-Ray Astronomy in Honour of Joachim Trmper's 65th Birthday, ed. B. Aschenbach & M. J. Freyberg (MPE Rep. 272; Garching: MPE), in press
- Wojdowski, P., Clark, G. W., Levine, A. M., Woo, J. W., & Zhang, S. N. 1998, ApJ, 502, 253

TABLE 1  
DIFFERENT PERIODS AND THEIR SIGNIFICANCES

Instrument (energy band)	Duration (days)	Periods (day) (false alarm prob.)	Periods in small segments (false alarm prob.)
<b>Cyg X-2</b>			
RXTE-ASM (1.5–12 keV)	1078	40.4 (1 E-20), 68.8 (7 E-25)	39.5 (4 E-9), 70.1 (1 E-12) 39.6 (9 E-6), 56.3 (7 E-8), 72.4 (3 E-7) 41.8 (2 E-7), 56.8 (5 E-7), 73.7 (1 E-10)
GINGA-ASM (1–20 keV)	1645	53.7 (1 E-4), 61.3 (1 E-7)	
ARIEL-5 (3–6 keV)	1963	41.3, 46.2, 53.9 <sup>a</sup> , 77.4 (1 E-16)	45.7 (3 E-3), 55.3 (1 E-5), 78 (0.9) <sup>b</sup> 43.2 (0.015), 68.6 (4 E-5), 78 (0.8) <sup>b</sup> 41 (0.025), 53 (1 E-4), 78 (0.07) <sup>b</sup>
VELA-5B (3–12 keV)	3675	33.9 (0.4), 77.4 (0.03)	
<b>LMC X-3</b>			
RXTE-ASM (1.5–12 keV)	1080	104 (3 E-38), 169 (2 E-27), 216 (1 E-28)	104 (3 E-27), 178 (2 E-35) 102 (6 E-12), 222 (1 E-11)
GINGA-ASM (1–20 keV)	1682	105 (1.5 E-3), 214 (1 E-10), 328 (2 E-5)	
HEAO 1 (1–13 keV)	506	99 (2 E-16), 203 (4 E-12)	
ARIEL-5 (3–6 keV)	1903	96 (8 E-3), 130 (0.03)	

<sup>a</sup>41.3 (1 E-15), 46.2 (7 E-20), 53.9 (2 E-23)

<sup>b</sup>In the periodograms generated from the segments of ARIEL 5 light curve, the peaks near 78 days are barely visible, but in the periodogram of the complete light curve it is highly significant (see Figure 2).